

Experimental analysis and large eddy  
simulation to determine the response of non  
premixed flame submitted to acoustic forcing

B. Varoquié\*<sup>†</sup>, J.P. L gier<sup>+</sup>, F. Lacas\*, D. Veynante\* and T. Poinsot<sup>+</sup>

\* Laboratoire E.M2.C.

C.N.R.S. - Ecole Centrale Paris

92295 CHATENAY-MALABRY CEDEX, FRANCE

<sup>+</sup>CERFACS

42, Av. G. Coriolis

31400 TOULOUSE CEDEX, FRANCE

<sup>†</sup>SNECMA

Division Moteur D partement YKC

77550 MOISSY CRAMAYEL

*Corresponding author* : Denis VEYNANTE

Laboratoire EM2C, CNRS - Ecole Centrale Paris

92295 Ch tenay-Malabry Cedex, France

Tel. : (33) 1 41 13 10 80

Fax : (33) 1 47 02 80 35

e-mail : denis@em2c.ecp.fr

*Keywords* : Turbulent non premixed combustion, large-eddy simulation,  
Combustion instabilities

*Colloquium topic* : Turbulent combustion

<i>Word length of this paper</i> : Text	2380	
Equations	168	(8 × 21)
References	140	(20 × 7)
Figures	2600	(4 × 400 + 5 × 200)
<b>Total</b>	<b>5288</b>	

submitted for *Oral Presentation* to the

*Twenty-Ninth International Symposium on Combustion*

*July 2002*

Experimental analysis and large eddy simulation to determine the response of  
non premixed flame submitted to acoustic forcing

**Abstract**

Large eddy simulations appear as a very promising tool to describe combustion instabilities but, as these instabilities generally involved acoustic waves through the whole system, relevant simulations are currently still impossible. An intermediate step is to use large eddy simulation of the burner only to estimate the parameters of the so-called  $n - \tau$  model where the flame is viewed as inducing an amplification  $n$  with the time delay  $\tau$  to the velocity perturbation. Then, these parameters are incorporated in a global acoustic model of the system to determine whether combustion instabilities may occur or not. The objective of this paper is to investigate the ability of large eddy simulations to determine the  $n - \tau$  parameter. An experimental turbulent nonpremixed flame is submitted to acoustic perturbations induced by loudspeakers. The flame transfer function is then determined and  $n$  and  $\tau$  are computed as a function of the downstream location in the burner.  $n$  and  $\tau$  are also extracted from large eddy simulations of the same burner submitted to velocity perturbations. The results are very promising because numerical and experimental data are in good agreement.

## Introduction

Combustion instabilities, due to a coupling between heat release, hydrodynamic flow field and acoustic waves, are encountered in various practical applications [1]. These instabilities have to be avoided because they induce noise, variations of the system characteristics, large heat transfers and may lead to the system destruction. The challenge for designers is to predict the possible occurrence of such instabilities and, if required, to avoid them, for example using passive or active control techniques [2]. Large Eddy Simulation (LES) appears today as a powerful tool to describe these instabilities, corresponding to large coherent structures resolved in the simulation, and to test control techniques [3, 4].

Unfortunately, combustion instabilities generally involve the complete system where from inlet to outlet and are still out of the present computer capabilities. An intermediate step is to use large eddy simulations to determine the flame transfer function by computing only the combustion chamber. This transfer function is then written in terms of the so-called  $n - \tau$  model proposed by Crocco [5] in his pioneering work. In this model, the flame is viewed as inducing a time delay,  $\tau$  and an amplification factor  $n$  on acoustic waves. The entire system is then decomposed in a series of acoustic elements having their own influence on acoustic waves. Once the full system is known, including acoustic boundary conditions, acoustic waves propagating in the system may be determined using simple codes (see [4] for a complete description). The main difficulty is then to determine the  $n - \tau$  model parameter for the flame. A possible approach is to determine the flame transfer function using LES. Numerical simulations of the combustion chamber are performed under inlet acoustic perturbations allowing the determination of the flame transfer function (i.e. the flame response to an acoustic perturbation). This approach is very attractive but needs validations against experimental data. In this paper, an experimental burner is used to determine these transfer functions

and results are compared to numerical simulations.

## The $n - \tau$ model for the flame transfer function

A one-dimensional discretization of a combustor is displayed on Fig. 1. Two combustor sections are considered. The first one (length  $L_1$ , section  $S_1$ , density  $\rho_1$  and sound speed  $c_1$ ) is filled with fresh gases and the second (length  $L_2$ , section  $S_2$ , density  $\rho_2$  and sound speed  $c_2$ ) contains burnt gases. The flame is supposed to be infinitely thin and lies in section  $x = L_1$ .  $A_1^+$ ,  $A_1^-$ ,  $A_2^+$ ,  $A_2^-$ , are the amplitudes of the waves travelling in downstream and upstream directions, respectively in sections 1 and 2. According to Ref. [4], wave amplitudes are linked through the system:

$$\begin{pmatrix} A_2^+ \\ A_2^- \end{pmatrix} = \frac{1}{2} \begin{bmatrix} e^{ik_1 L_1} (1 + \Gamma_1) & e^{-ik_1 L_1} (1 - \Gamma_1) \\ e^{ik_1 L_1} (1 - \Gamma_1) & e^{-ik_1 L_1} (1 + \Gamma_1) \end{bmatrix} \begin{pmatrix} A_1^+ \\ A_1^- \end{pmatrix} + \frac{1}{2} \frac{\rho_2 c_2}{S_2} \begin{pmatrix} +\frac{\gamma-1}{\rho_1 c_1^2} \Omega \\ -\frac{\gamma-1}{\rho_1 c_1^2} \Omega \end{pmatrix} \quad (1)$$

where  $\Gamma_1 = (\rho_2 c_2 S_1) / (\rho_1 c_1 S_2)$ .  $k_1$  is the wave number  $k_1 = \omega / c_1$  where  $\omega$  is the wave pulsation.  $\gamma$  is the ratio of constant pressure and constant volume heat capacities, assumed to be constant, and  $\Omega$  the source term due to combustion. System (1) must be solved for the wave amplitudes  $A_1^+$ ,  $A_1^-$ ,  $A_2^+$ ,  $A_2^-$  and the pulsation  $\omega$  using additional boundary conditions. In the  $n - \tau$  model, the oscillatory combustion is produced by perturbation of the velocity at the flame ( $x = L_1$ ) with a time delay  $\tau$ . The source term  $\Omega$  becomes:

$$\frac{\gamma-1}{\rho_1 c_1^2} \Omega = S_1 n u(L_1, t - \tau) \quad (2)$$

where  $n$  is the interaction index and has no dimension and  $u(x, t)$  the axial velocity at location  $x$  and time  $t$ . The previous relation may be rewritten in the spectral

space:

$$\frac{\gamma-1}{\rho_1 c_1^2} \widehat{\Omega}(f) = S_1 n \widehat{u}(L_1, f) \quad (3)$$

where  $f$  is the frequency and  $\widehat{Q}$  denotes the Fourier transform of the function  $Q$ . In terms of wave amplitudes, Eq. (2) may be rewritten:

$$\frac{\gamma-1}{\rho_1 c_1^2} \Omega = \frac{n}{\rho_1 c_1} S_1 e^{i\omega\tau} (A_1^+ e^{ik_1 L_1} - A_1^- e^{-ik_1 L_1}) \quad (4)$$

This model requires the knowledge of  $n$  and  $\tau$ . In the following, experimental determination of these parameters are compared to values extracted from large eddy simulations of the burner.

## Experimental setup

The combustion chamber is specially designed both for easy optical diagnostics (two dimensional configuration) and easy numerical simulations (simple grid meshes). Propane is injected through two slots in a coflowing air stream (Fig. 2 and 3). Two backward facing steps ensure the flame stabilization. The burner is 300 mm in length, 80 mm in width and 100 mm high. Depending on the fuel and air flow rates, the turbulent flame may be anchored in the vicinity of the propane injectors (Fig. 4a), lifted and stabilized by the recirculation zones induced by the facing steps (Fig. 4b) or blown-off [6].

In order to investigate the flame response to longitudinal acoustic perturbations, the air flow is modulated by plane waves induced by two loudspeakers plugged in the inlet duct. The maximum frequency of the acoustic forcing was chosen below the frequency of the first transverse mode of the combustion chamber (i.e.  $f_t = 1307$  Hz) to ensure that only longitudinal modes interact with the flame. In our case, the air flow was never forced at frequency over 500 Hz. The

transfer function characterizes the flame response to velocity and pressure periodic disturbance of the air flow. Velocity variations are measured 17 mm upstream the combustion chamber inlet using an hot-wire anemometer located in this air duct on the symmetry axis (Fig. 3). The heat release fluctuations are estimated from the  $CH$  radical emission measured by a photomultiplier and a narrow band filter centered around 434 nm. The axial velocity at the burner inlet is imposed by acoustic excitation as  $u(L_1, t) = U_0 + A \sin(2\pi ft)$  with  $U_0 = 24$  m/s and  $A = 0.05 U_0$ .

In the lifted flame regime (Fig. 4b) investigated here (propane flow rate: 4.5 g/s, air flow rate: 75 g/s, leading to a global equivalence ratio  $\phi = 0.81$ ), reactants are partially mixed before reaching the flame. Hurle [7] had shown that, for a given equivalence ratio,  $CH$  emission is proportional to heat released rate but the equivalence ratio variation is not monotonous to  $CH$  emission when the reactant flow rates are modified. However, normalizing the emission signal using its stoichiometric value, the error remains small when a bijection is assumed between  $CH$  emission and heat release rate [8]. In fact, for low variations of the equivalence ratio around the stoichiometric value ( $0.8 \leq \phi \leq 1.2$ ), this error does not exceed 15 percent and the  $CH$  radical emission is relevant to measure the reaction heat release rate.

$CH$  radical emissions are measured using a 10 mm width vertical slot moving along the axis of the combustion chamber (Fig. 3), allowing a spatial analysis of the flame transfer function. Relations (2) and (3) still hold but the time delay  $\tau$  and the interaction index  $n$  become functions of the downstream location  $x$ .  $n_x$  and  $\tau_x$  are determined using Fourier transforms of the velocity and  $CH$  radical emission signals using Eq. (3). The local time delay  $\tau_x$ , is the time needed for a velocity perturbation at the burner inlet to interact with the flame whereas the local interaction index,  $n_x$ , reveals the spatial location of the flame response in the burner.

## Experimental results

Various acoustic frequencies, belonging both to the rig longitudinal modes range and to the natural low frequency broad band noise in the combustion chamber, have been experimentally tested. Acoustic forcing at  $f_e = 170$  Hz, 200 Hz and 350 Hz induces the highest coherence function between the axial velocity signal and the heat release rate. The local index  $n_x$  is plotted versus the downstream location  $x$  for the three excitation frequencies on Fig. 5. The  $n_x$  maximum value is obtained around the middle of the combustion chamber for the two low frequencies while this value for the 350 Hz forced case is slightly shifted downstream and less important. Moreover, the 350 Hz forced case presents a better interaction near the burner inlet but the interaction is globally less important. The flame appears to be more sensitive to low frequencies and the difference between 170 Hz and 200 Hz seems to be negligible.

This finding may be explained by computing the most amplified mode of the mixing layer  $f_0$  and the cut-off frequency  $f_n$  as [9]:

$$f_0 = 0.035 \frac{\bar{U}_m}{\theta}, \quad f_n = 0.08 \frac{\bar{U}_m}{\theta}, \quad \bar{U}_m = \frac{\rho_{C_3H_8} \bar{U}_{C_3H_8} + \rho_{air} \bar{U}_{air}}{\rho_{C_3H_8} + \rho_{air}} \quad (5)$$

where

$$\theta = \frac{1}{(\bar{U}_{C_3H_8} - \bar{U}_{air})^2} \int_0^E (\bar{U}_{C_3H_8} - U(y))(U(y) - \bar{U}_{air}) dy \quad (6)$$

is the momentum thickness of the mixing layer.  $U_m$  is the mean axial velocity and  $E$  the injection half high (15 mm).  $\rho_{C_3H_8}$ ,  $\bar{U}_{C_3H_8}$ ,  $\rho_{air}$  and  $\bar{U}_{air}$  are respectively the density and the velocity of propane and air streams. Mean axial velocity and momentum thickness are estimated using particle image velocimetry (PIV) data (Fig. 6). In our case,  $\theta=0.0013$  m,  $f_0=230$  Hz and  $f_n=527$  Hz, so excitation frequencies 170 Hz and 200 Hz are close to the most amplified frequency  $f_0$  of the mixing layer, leading to an organized flame structure at these frequencies. On

the other hand,  $f_e = 350$  Hz is closer to the cut-off frequency  $f_n$  and the mixing layer is less affected by the acoustic excitation.

The local time delay  $\tau_x$  is plotted as a function of the downstream location  $x$  on Fig. 7. This delay is estimated using the coherence function between velocity and heat release measurements (Fig. 8) to ensure a correct phase unwrapping. As the three points closest to the burner inlet present low coherence value (Fig. 8), the unwrapping technique in this case is not meaning full. In fact, the heat release rate is probably dominated in this region by the unsteady phenomena in the recirculation zones and is not directly related to the inlet velocity. The local time delay  $\tau_x$  has been unwrapped from the 4<sup>th</sup> point ( $x \approx 40$  mm). The delay  $\tau_x$  versus  $x$  is proportional to the convection velocity of reactive structure in the combustion chamber. The variations in the slope of  $\tau_x$  versus  $x$  show that reactive structures are y convected more rapidly when the frequency decreases. This trend is also confirmed by the mixing layer stability analysis: when the velocity perturbations frequency is shifted from  $f_0$  towards the cut-off value  $f_n$  the phase velocity of vorticity waves moves from  $\bar{U}_{C_3H_8}$  to  $\bar{U}_m$ . The reference convection delay plotted on figure 7 corresponds to a  $\bar{U}(L_1) = 24ms^{-1}$  axial velocity value ( $\tau_{x=x}/\bar{U}(L_1)$ ).

## Comparison between LES results and experimental data

The objective is now to investigate the ability of large eddy simulation to reproduce the time delay  $\tau_x$  and the interaction index  $n_x$ . Large eddy simulations of the burner are performed modeling unresolved Reynolds stresses using the filtered Smagorinsky model [10] and describing the combustion by the dynamically thickened flame model (DTFLES, see [11]). The flame front cannot be resolved in LES and the combustion is mainly a subgrid scale phenomenon. Following [12],

the flame thickness may be increased by a factor  $F$  keeping constant the laminar flame speed by increasing molecular diffusivities by a factor  $F$  and decreasing the reaction rate by the same factor  $F$ . To account for the flame turbulence interaction at the subgrid scale level Colin *et al.* [13] have developed an efficiency function,  $E$ , depending on the turbulence and flame characteristics. L egier *et al.* [11, 6] have also shown that the thickening factor  $F$  may depend on the spatial location. Then, the flame is thickened by increasing  $F$  in the reaction zone whereas outside the flame, the molecular mixing is unaffected keeping  $F = 1$ . The final balance equation for the fuel mass fraction  $Y_F$  is, using classical notations:

$$\frac{\partial \bar{\rho} \tilde{Y}_F}{\partial t} + \nabla \cdot (\bar{\rho} \tilde{\mathbf{u}} \tilde{Y}_F) = \nabla \cdot (\bar{\rho} (\mathcal{D}FE + D_t) \nabla \tilde{Y}_F) - \frac{E}{F} \dot{\omega}_F \quad (7)$$

where  $\bar{\rho}$ ,  $\tilde{\mathbf{u}}$  and  $\tilde{Y}_F$  denotes resolved density, velocity field and fuel mass fraction respectively.  $D_t$  is the turbulent diffusivity and the reaction rate  $\dot{\omega}_F$  is expressed using an Arrhenius law based using resolved mass fractions and temperature. This model is implemented in the AVBP code developed at CERFACS. The numerical scheme is third order both in space and time [14] and NSCBC boundary conditions [15] are used. As a first step, two dimensional simulations are performed. Numerical simulations of the steady state operating regimes have reproduced turbulent flame stabilization modes (i.e. ‘‘anchored’’, ‘‘lifted’’ or blow-off [11][6]). **In fact, these simulations are quite expensive, especially when the frequency of the acoustic excitation is low. Our code is fully compressible and should fit the CFL criterion but relevant data are only achieved when a several periods are simulated. This is the reason why 170 Hz and 350 Hz excitation frequencies have not been simulated. We have preferred to investigate the implication of 2D versus 3D simulations (LES should theoretically be performed in 3D) and to analyze if the discrepancies observed between numerical simulations and experimental data may be explained by three dimensional motions. This point is still under investigation. In the present simulations, the burner veloc-**

**ity inlet is modulated to 200 Hz according to experimental acoustic excitation. 900000 iterations, corresponding to about 20 acoustic cycles, have been performed leading to 320 hours in terms of CPU time on a IBM SP3 parallel computer.**

Heat release rates as a function of the downstream location  $x$  are estimated as in the experiment by integration over vertical slots (Fig. 3). The scaling between the photomultiplier signal and the heat release rate has been done assuming that: 1) the propane burns homogeneously inside the combustion chamber (i.e. the same amount of fuel burns in each slot). This assumption is rough but the emission rms over the thirty slots does not exceed 20 % of the mean signal. 2) non linear variation between the  $CH$  radical emission and the heat release rate are neglected.

Numerical simulations and experimental data for the interaction index  $n_x$  and the time delay  $\tau_x$  are compared on Fig. 9. The agreement is very good and the numerical simulations are able to reproduce both  $\tau_x$  and  $n_x$ . The convection of the perturbation is well captured by the model and the maximum variation obtained between measured and computed  $\tau_x$  is less than the acoustic period  $1/f_e = 5$  ms. At  $x = 50$  mm downstream of the inlet, the interaction index  $n_x$  extracted from the LES is larger than the experimental data. Nevertheless, recent results show that this discrepancy is apparently not observed when performing three-dimensional large eddy simulations and could be due to 3D motions in the flow field.

## Conclusion

A turbulent nonpremixed propane/air flame is submitted to acoustic perturbations induced by loudspeakers to characterize the flame transfer response in terms of an interaction index  $n$  (amplification factor) and a time delay  $\tau$  (phase shift relatively to the inlet velocity perturbation), as a function of the downstream location in

the burner  $x$ .  $n$  and  $\tau$  are the parameters of the so-called  $n - \tau$  model proposed by Crocco to describe combustion instabilities. Large eddy simulations of the same burner submitted to inlet velocity perturbations are also performed, using the Dynamic Thickened Flame Model (DTFLES). Parameters  $n$  and  $\tau$  are also extracted from the simulations and compared to experimental data. The agreement is very good and large eddy simulations appear to be a very promising tool to extract flame transfer functions required in global acoustic description of the full system.

## Acknowledgments

The financial supports by SNECMA and European Union (ICLEAC Contract) are gratefully acknowledged.

## References

- [1] Crocco, L. and Cheng, S. *Theory of combustion instability in liquid propellant rocket motors*, volume Agardograph No 8. Butterworths Science, 1956.
- [2] McManus, K., Poinso, T., and Candel, S. *Prog. Energ. Combust. Sci.*, 19:1–29 (1993).
- [3] Menon, S. and Jou, W. *Combustion, Science and Technology*, 75(1-3):53 – 72 (1991).
- [4] Poinso, T. and Veynante, D. *Theoretical and numerical combustion*. Edwards, 2001.
- [5] Crocco, L. *J. Aero. Res. Soc.*, 21 & 22 (1952).

- [6] Légier, J., Poinso, T., Varoquié, B., Lacas, F., and Veynante, D. *Symposium on Turbulence Mixing and Combustion*, pages 271 – 278. IUTAM, 2001.
- [7] Hurle, I., Price, R., Sugden, T., and Thomas, A. *Proc.Roy.Soc.London A*,303-409, (1968).
- [8] Samaniego, J. PhD thesis, Ecole Centrale Paris, laboratoire EM2C, 1992.
- [9] Trouvé, A. PhD thesis, Ecole Centrale Paris, laboratoire EM2C, 1989.
- [10] Ducros, F., Nicoud, F., and Schönfeld, T. *Eleventh Symposium on Turbulent Shear Flows*, Grenoble, France, 1997.
- [11] Légier, J., Veynante, D., and Poinso, T. *Proceedings of the Summer Program*. Center for Turbulence Research, 2000.
- [12] O'Rourke, P. and Bracco, F. *J. Comp. Phys.*, 33(2):185–203 (1979).
- [13] Colin, O., Ducros, F., Veynante, D., and Poinso, T. *Phys. Fluids A*, 12(7):1843 – 1863 (2000).
- [14] Colin, O. and Rudgyard, M. *J. Comp. Phys.*, 162:338 – 371 (2000).
- [15] Poinso, T. and Lele, S. *J. Comp. Phys.*, 101(1):104–129 (1992).

## List of Figures

1	One-dimensional discretization of harmonic acoustic wave in a combustor. The flame is assumed to be thin and lies at $x = L_1$ . . .	15
2	Experimental setup . . . . .	15
3	A detailed view of the combustion chamber . . . . .	16
4	Combustion regimes visualized using $CH$ radical spontaneous emission, gray scale values correspond to the mean reaction rate whereas contour lines display the reaction rate fluctuations. (a): “anchored flame” regime. The flame is stabilized in the vicinity on the fuel injectors but is not anchored on the lips. (b) “lifted flame” regime where the flame is stabilized by recirculation zones induced by the two backward facing steps. . . . .	16
5	Local interaction index $n_x$ (Eq. 2) plotted as a function of the downstream location $x$ for the three excitation frequencies $f_e = 170$ Hz, 200 Hz and 350 Hz. . . . .	17
6	Mean axial velocity profile at the burner inlet, obtained from particle image velocimetry (PIV) and used to estimate the initial momentum thickness $\theta$ of the air/propane mixing layer (Eq. 6). . . .	18
7	Local time delay $\tau_x$ plotted as a function of the downstream location $x$ for the three excitation frequencies. The reference convective delay corresponds to a convection velocity equal to 25 m/s. . .	19
8	Coherence function between velocity and heat release rate (radical $CH$ emission) for the three excitation frequencies plotted as a function of the downstream location $x$ . . . . .	20
9	Comparison between large eddy simulations using the TFLES model and experimental data. Top: interaction index $n_x$ ; bottom: time delay $\tau_x$ . . . . .	21

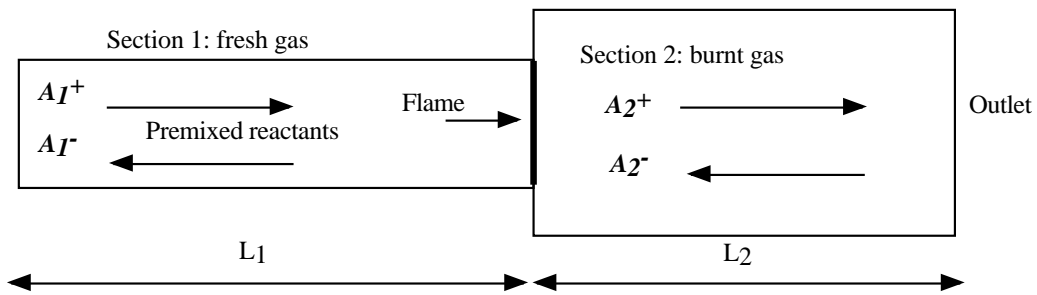


Figure 1: One-dimensional discretization of harmonic acoustic wave in a combustor. The flame is assumed to be thin and lies at  $x = L_1$ .

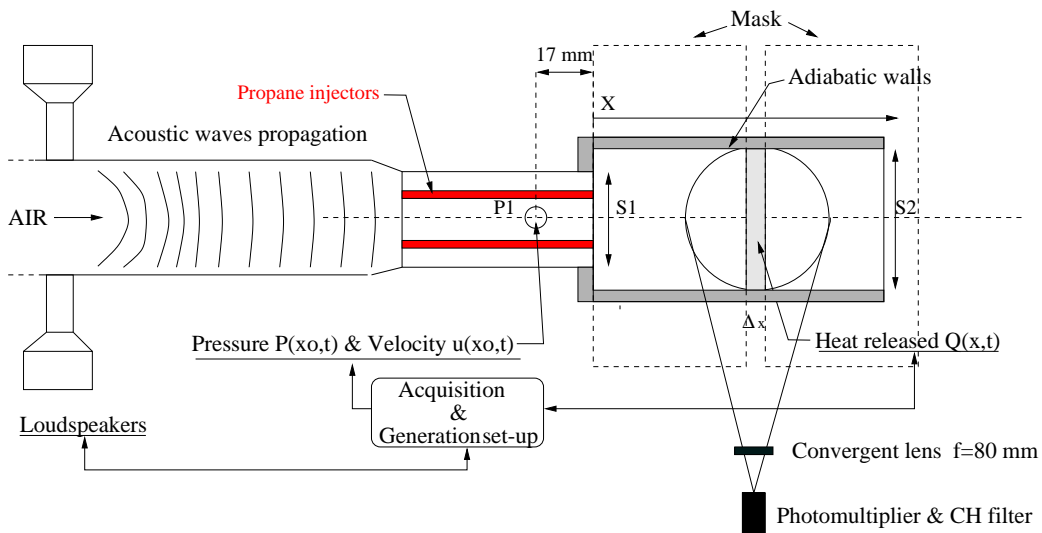


Figure 2: Experimental setup

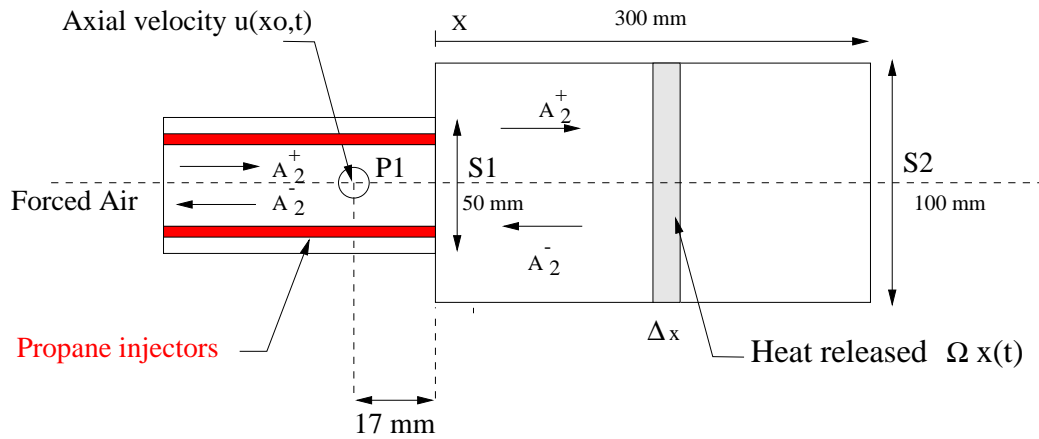


Figure 3: A detailed view of the combustion chamber

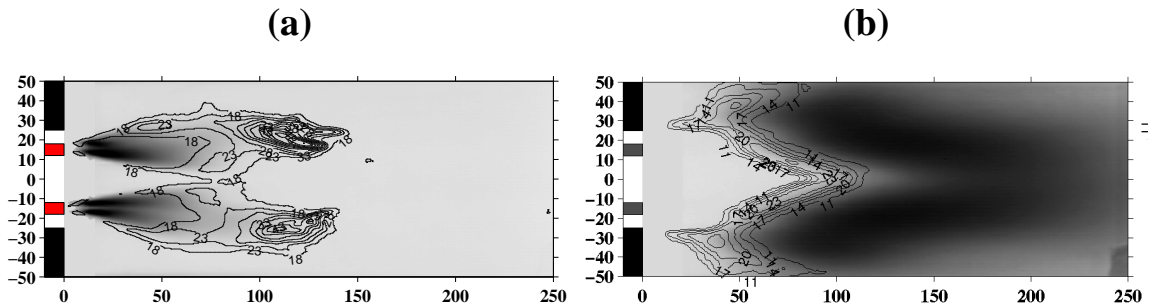


Figure 4: Combustion regimes visualized using  $CH$  radical spontaneous emission, gray scale values correspond to the mean reaction rate whereas contour lines display the reaction rate fluctuations. (a): “anchored flame” regime. The flame is stabilized in the vicinity on the fuel injectors but is not anchored on the lips. (b) “lifted flame” regime where the flame is stabilized by recirculation zones induced by the two backward facing steps.

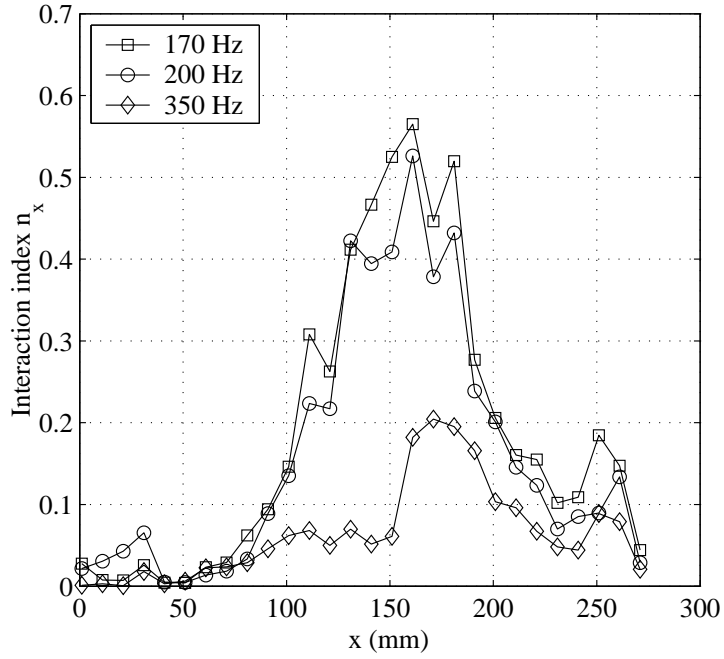


Figure 5: Local interaction index  $n_x$  (Eq. 2) plotted as a function of the downstream location  $x$  for the three excitation frequencies  $f_e = 170$  Hz, 200 Hz and 350 Hz.

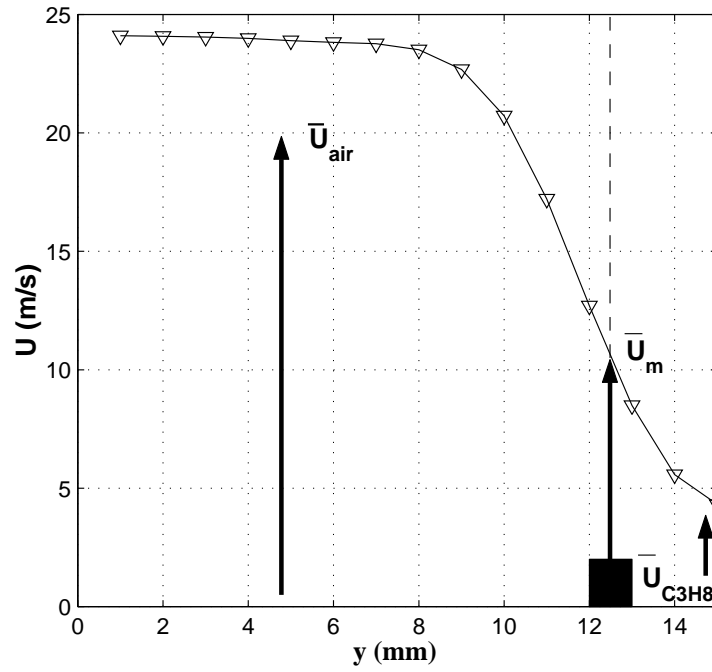


Figure 6: Mean axial velocity profile at the burner inlet, obtained from particle image velocimetry (PIV) and used to estimate the initial momentum thickness  $\theta$  of the air/propane mixing layer (Eq. 6).

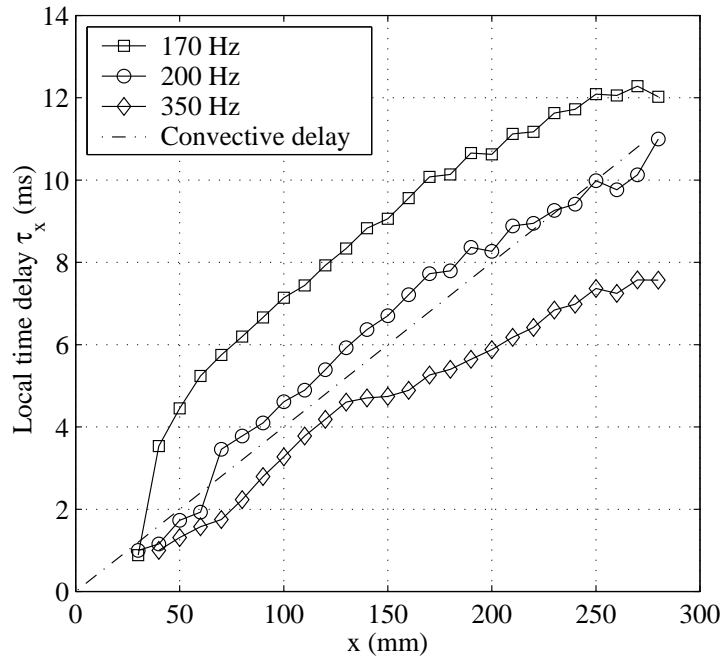


Figure 7: Local time delay  $\tau_x$  plotted as a function of the downstream location  $x$  for the three excitation frequencies. The reference convective delay corresponds to a convection velocity equal to 25 m/s.

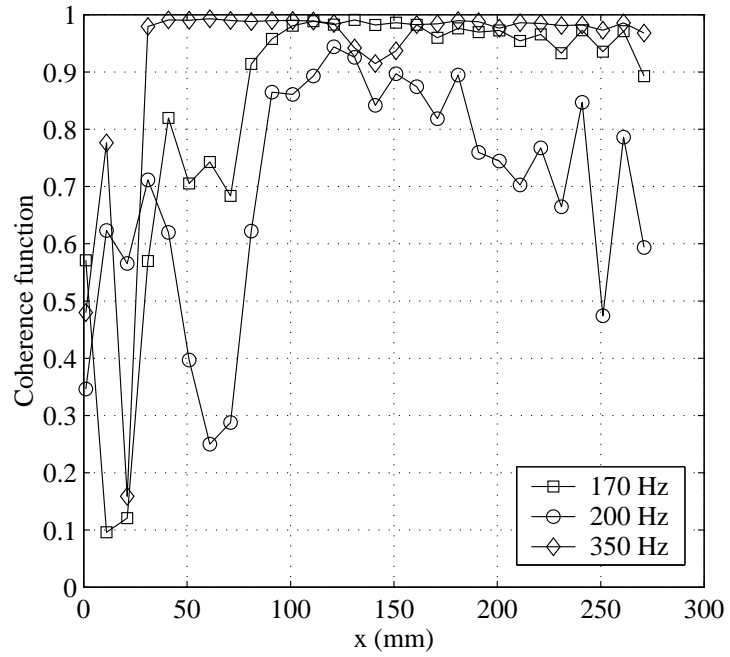


Figure 8: Coherence function between velocity and heat release rate (radical  $CH$  emission) for the three excitation frequencies plotted as a function of the downstream location  $x$ .

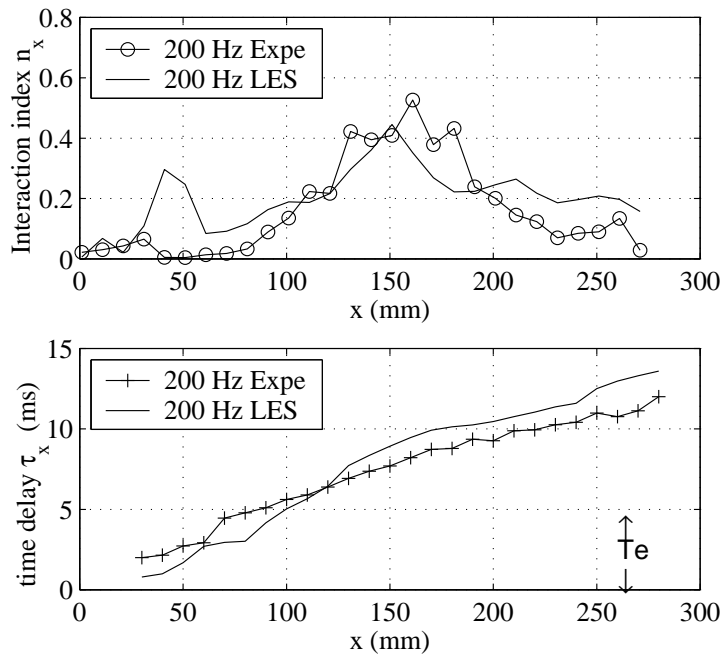


Figure 9: Comparison between large eddy simulations using the TFLES model and experimental data. Top: interaction index  $n_x$ ; bottom: time delay  $\tau_x$ .